# An Analysis on Optimal Cluster Ratio in Cluster-Based Wireless Sensor Networks

Zilong Jin, *Student Member, IEEE*, Dae-Young Kim, Jinsung Cho, *Member, IEEE*, and Ben Lee, *Member, IEEE*

***Abstract*— In wireless sensor networks, clustering schemes have been adopted as an efficient solution to prolong the network lifetime. In these schemes, the performance of energy-efficient data transmission is affected the cluster ratio (CR). This paper analyzes the optimal CR from the perspective of network energy efficiency, and its impact on the network lifetime. In order to provide a generic analytic model, various data propagation cases are mathematically analyzed. In addition, the network lifetime is extended by jointly optimizing the network transmission count and link reliability. Our simulation results show that the optimal CR derived based on the proposed analytical model enhances the energy efficiency and effectively increases the network lifetime.**

***Index Terms*— Wireless sensor network, cluster ratio, inherent transmission count, packet reception ratio, network lifetime.**

## I. Introduction

A WIRELESS Sensor Network (WSN) is a multi-hop based network that allows sensor devices to communicate without any network infrastructure. It consists of a large number of tiny sensor nodes each equipped with a microprocessor, a memory, sensing modules, radio transceivers, and a battery. WSNs are widely deployed in environment monitoring, healthcare, intrusion detection, etc., and play a key role in the Internet of Things (IoT) paradigm. However, sensor nodes have limited battery power, and therefore, energy efficiency is crucial for prolonging the network lifetime of WSNs.

In order to prolong the network lifetime, many schemes have been proposed with energy efficiency in mind, such as energy efficient Media Access Control (MAC) and routing schemes. Furthermore, some research efforts have been made on exploring energy efficient network architectures. For example, Heinzelman *et al.* proposed a cluster-based communication protocol called Low-Energy Adaptive Clustering Hierarchy (LEACH) [1], which is the most well-known clustering scheme for WSNs. Recently, clustering schemes have been explored to enhance energy efficiency and communication performance, as well as improve network scalability [2]–[6]. Clustering schemes in WSNs can decrease the amount of transmitted traffic at a Cluster Head (CH) using data aggregation, and thus energy can be saved during data transmission [7]. In addition, since nodes are managed as a cluster, the network becomes more robust and the overhead due to frequent topology changes is reduced.

Prior research efforts in cluster-based WSNs [1], [8]–[10], [16]–[19] indicate the importance of *Cluster Ratio* (*CR*), which is the ratio of the number of cluster-heads and the total number of nodes. These studies found that an improper choice of *CR* will result in extra energy dissipation, and thus an appropriate choice of *CR* is critical for enhancing the network lifetime. However, their results are only based on specific environments and transmission cases, and thus not applicable for general cluster-based WSNs. For example, Yang and Sikdar [8] and Chen *et al.* [9] proposed analytical models to determine the optimal *CR*, but they do not consider multi-hop transmissions. Xie and Jia [19] mathematically analyzed the optimal *CR* for minimizing the number of network transmissions. Their analysis was performed based on the assumption that the network is divided into uniformed sized clusters. However, this is not the case in most WSN applications, where the location and shape of each cluster are random. Consequently, there are no valid analytical models that can be applied using generic assumptions and various data propagation cases.

This paper analyzes the relationship between *CR* and network performance for improving the network energy efficiency. This is achieved by modeling a cluster-based WSN as a 2-dimensional Poisson point process and analyzing the impact of *CR* on the network performance in terms of transmission count and *Packet Reception Ratio* (*PRR*). Then, a joint optimization scheme is proposed to derive the optimized *CR* that guarantees network energy efficiency and prolongs network lifetime.

The specific contributions of this paper are as follows:

- The impact of *CR* on the network performance is mathematically analyzed in terms of transmission count and communication reliability.
- The optimal *CR* is analyzed for a generic and feasible network environment as well as various data propagation cases. This allows the proposed analytic model and the result of optimal *CR* to be widely applied in cluster-based WSNs.
- An important ***Theorem*** and an accompanying proof are provided to show that the inherent transmission count of a cluster-based WSN is a ***Convex Function*** of *CR*.

Manuscript received June 4, 2015; revised July 9, 2015; accepted July 16, 2015. Date of publication July 21, 2015; date of current version September 4, 2015. This work was supported by the Basic Science Research Program through the National Research Foundation of Korea within the Ministry of Education under Grant NRF-2013R1A1A2059741. The associate editor coordinating the review of this paper and approving it for publication was Prof. Elena Gaura.

Z. Jin and J. Cho are with the Department of Computer Engineering, Kyung Hee University, Yongin 446-701, Korea (e-mail: jinzilong@khu.ac.kr; chojs@khu.ac.kr).

D.-Y. Kim is with the Department of Software Engineering, Changshin University, Changwon 630-764, Korea (e-mail: dyoung.kim81@gmail.com).

B. Lee is with the School of Electrical Engineering and Computer Science, Oregon State University, Corvallis, OR 97331 USA (e-mail: benl@eecs.orst.edu).

Color versions of one or more of the figures in this paper are available online at http://ieeexplore.ieee.org.

Digital Object Identifier 10.1109/JSEN.2015.2459374

(The definition for inherent transmission count will be given in Sec. IV.) This property indicates that the network energy efficiency can be guaranteed by optimizing *CR*.
- A joint optimization is performed to simultaneously optimize transmission count and *PRR*. The optimized results are verified using simulation.

The rest of the paper is organized as follows: Sec. II discusses the most relevant related work. The system model under consideration is discussed in Sec. III. Sec. IV formulates the optimal *CR* problem, and proposes an analytical model for various data propagation cases. A set of simulation results and analyses are presented in Sec. V. Finally, Sec. VI concludes the paper and discusses possible future work.

## II. Related Work

LEACH is one of the earliest proposed hierarchical routing protocol that utilizes local CHs operating as routers to the sink node [1]. In addition, it uses an energy efficient clustering scheme that forms nodes into clusters based on received signal strength. Before starting the LEACH algorithm, an initial *CR* value needs to be defined. Then, CHs are selected according to a threshold value calculated based on the initial *CR* value. However, the selection of CHs is random, and thus balanced energy consumption among all the nodes is not guaranteed.

A number of methods have been proposed with the aim of solving the drawbacks of LEACH and to further improve network energy efficiency [8]–[10]. The closest one is LEACH-E [10], which improves the optimal *CR* calculation and the cluster formation scheme to balance the energy consumption among CHs. However, the optimal *CR* values obtained in these methods are confined to clustering with direct transmission, which suffers from high energy-cost required to perform long distance transmissions. In practice, sensor nodes have limited battery power; therefore, the results from the LEACH-based analyses cannot be directly applied to most applications.

Due to the high cost of long distance transmissions, Younis *et al.* proposed the Hybrid, Energy-Efficient and Distributed (HEED) clustering scheme [11], which adopts multi-hop, inter-cluster communication and improves the CH selection scheme of LEACH to balance energy consumption. However, they did not quantitatively analyze the optimal *CR* value, and instead adopted the optimal *CR* result from LEACH as their initial *CR* value and discussed the required *CR* based on the cluster radius which is a random value. Wei *et al.* aim to relieve the relay load of CHs, which increases as the distance to the sink node decreases [12]. In order to achieve balanced load among CHs, the cluster size is determined based on the distance between a CH and the sink node. Manisekaran *et al.* proposed an energy efficient cluster formation scheme that selects a CH based on data sending rate and redundancy [14]. However, the authors do not provide any mathematical model to analyze the impact of *CR* on the network performance.

There is only a limited work that mathematically argues the impact of *CR* on the network performance. Kim *et al.* [15], Kumar *et al.* [16], and Kumar [17] show the importance of optimal *CR* on network performance, and extend the optimal *CR* analysis in LEACH to multi-hop transmissions using different performance metrics. However, a limitation of these efforts is that their analyses are performed based on specific energy models, and thus their results cannot be applied to different network environments. Therefore, their analytical models for optimal *CR* do not reveal the vital relationship between *CR* and network performance.

Bandyopadhyay and Coyle [18] proposed an analytical model that is derived based on a general energy model. In their work, the optimal *CR* is obtained by minimizing the network transmission count. However, the approximation applied to their analysis introduces additional calculation errors, and packet retransmission is not considered. Therefore, the optimized *CR* derived using their analytical model will not efficiently enhance the network lifetime. Xie and Jia [19] proposed an analytical model, which is independent of energy models, to analyze the optimum value for *CR*. Their analytic model is derived based on the assumption that the network is uniformly divided by clusters. However, this assumption is not generic for most WSN applications, where the location and shape of each cluster are random.

Based on analyzing the features of the existing analytic models discussed above, it is clear that none of these can be efficiently applied in cluster-based WSNs. To fill this gap, this paper first mathematically analyzes the impact of *CR* on the network performance. Then, an efficient analytic model is proposed and used to derive the optimal *CR* value for a generic and feasible network environment where the locations of sensor nodes and clusters are random. In order to allow the analytic model to guarantee network energy efficiency, a joint optimization is performed in terms of inherent transmission count and communication reliability.

## III. System Model

In order to quantitatively analyze the impact of *CR* on the network performance, this section presents the cluster model, the data propagation model, and the signal propagation model.

### A. Cluster Model

Our cluster model is based on the assumption that sensor nodes are deployed in a network area $A$ using a 2-dimensional Poisson point process with intensity $\lambda$. The network contains several clusters and each cluster is managed by a *Cluster Head* (CH). The CHs are selected based on a predetermined *CR*. In addition to CHs, the other nodes, called *Cluster Members* (CMs), join the CH that is closest to them. The resulting cluster-based network can be regarded as a Voronoi tessellation, where each cluster is a Voronoi cell [20], [21]. Foss *et al.* presented stochastic geometry properties of a Voronoi cell [21]. This paper models the cluster-based network by extending these properties. In order to achieve this, the following parameters are defined:

- $p$: Cluster ratio defined as $p = \frac{N_{CH}}{N}$, where $N_{CH}$ and $N$ represent the number of CHs and total number of nodes, respectively.
- $\lambda_{CH}$: The density of CH defined as $\lambda_{CH} = \frac{N \times p}{A} = \frac{N_{CH}}{A}$.

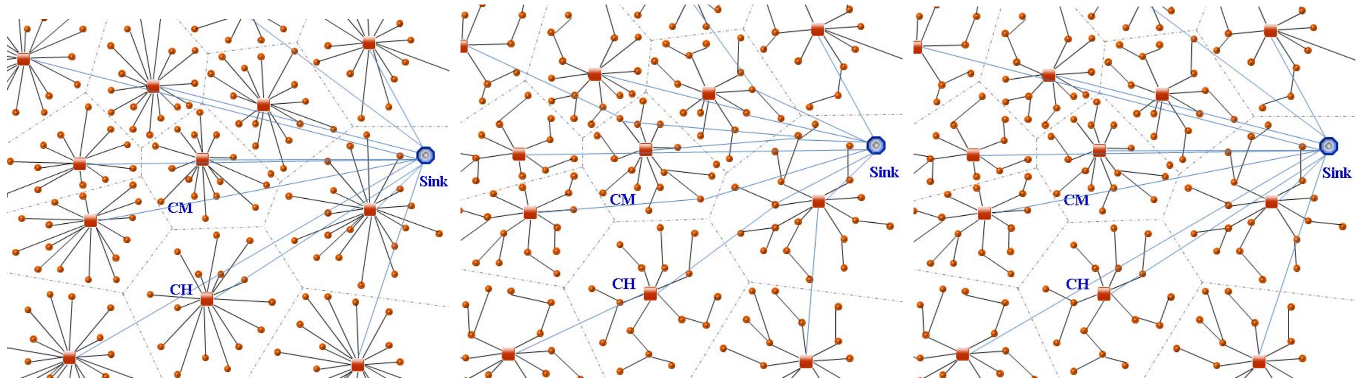


(a) (b) (c)

Fig. 1. Data propagation models. (a) *s2s* case. (b) *m2m* case. (c) *m2s* case.

- $\lambda_{CM}$: The density of CM defined as $\lambda_{CM} = \lambda(1-p)$
- $r$: Transmission radius of a node.

### B. Data Propagation Model

This paper classifies intra- and inter-cluster data propagation as either direct or multi-hop. Fig. 1 shows the three data propagation models in cluster-based WSNs. CMs transmit sensed data to their CH either directly or using multi-hop, which is also the case for communications between CHs and the sink node. Fig. 1a shows the *single-hop to single-hop* (*s2s*) case, where data propagation within intra-cluster and inter-cluster is performed using direct transmission. Prior research has shown that when the network range is wide, the energy consumption for *s2s* data transmission is excessive, and thus not applicable in most WSN applications. Therefore, this data propagation model is not considered in our analysis. Fig. 1b shows the *multi-hop to multi-hop* (*m2m*) case, where data propagation is performed using multi-hop transmission with short intra-cluster and inter-cluster communications. Finally, Fig. 1c shows the *multi-hop to single-hop* (*m2s*) case, which reduces the energy consumed by the nodes that are near to the sink node by employing long-range, low-power RF module (such as low-power Buletooth) to support direct transmission between CHs and the sink node. Therefore, data propagation is performed using multi-hop transmission with short intra-cluster communications and direct transmission with long distance inter-cluster communications.

### C. Signal Propagation Model

The signal propagation model is based on the *log-normal shadowing path-loss model*, which provides a relatively accurate channel model for WSNs. The path-loss model *PL* is represented as

$$PL(d) = PL(d_0) + 10\mu \log_{10}\left(\frac{d}{d_0}\right), \tag{1}$$

where $d$ denotes the distance between a sender and a receiver, $d_0$ is a reference distance, and $\mu$ is the path loss exponent. IEEE Std. 802.15.4 specifies a two-segment function for the path-loss model, and defines $\mu = 2.0$ for the first 8 $m$ and then $\mu = 3.3$ for the rest [25]. Therefore, the path-loss model of IEEE Std 802.15.4 is represented as

$$PL(d) = \begin{cases} PL(d_0) + 10\mu \log_{10}\big(d\big) & d \le d_0^{'} \\ PL(d_0^{'}) + 10\mu \log_{10}\left(\dfrac{d}{d_0^{'}}\right) & d > d_0^{'}, \end{cases} \tag{2}$$

where $d_0 = 1\ m$, $d_0^{'} = 8\ m$, $\mu = 2$ if $d \le d_0^{'}$, and $\mu = 3.3$ if $d > d_0^{'}$. The path loss at the reference distance ($d_0$) is given by

$$PL(d_0) = 10\mu \log_{10}\left(\frac{4\pi d_0 f}{C}\right), \tag{3}$$

where $f$ is the signal frequency and $C$ is the speed of light.

## IV. Analysis of Optimal Cluster Ratio

In a sensor device, energy is mainly consumed by the computational component and the RF module. Akyildiz *et al.* showed that the energy consumption of the RF module is 10 times that of the computational component [2]. Therefore, energy efficiency in WSNs is mainly constrained by the number of wireless communications consisting of both transmissions and retransmissions. For this reason, our objective is to improve the network energy efficiency by minimizing the number of inherent transmissions and retransmissions.

Sec. IV-A mathematically analyzes the impact of *CR* on the inherent transmission count of a network. Sec. IV-B explores the impact of *CR* on Packet Reception Ratio (*PRR*) to maximize communication reliability. Finally, Sec. IV-C presents a joint optimization scheme to derive the optimal *CR*, which simultaneously optimizes both the inherent transmission count and the communication reliability, i.e., *PRR*.

### A. Optimal Cluster Ratio for Minimizing Inherent Transmission Count

In this paper, a densely deployed network is assumed in which the sensor nodes' connectivity can be guaranteed. This is a fair assumption because the node density in sensor network applications tends to be higher than the minimum node density requirement, which is just enough to guarantee the network connectivity to provide network redundancy and to make sure that a point in a region of interest can be sensed by more than one sensor node [22]–[24]. Furthermore, in order to analyze and quantify the transmission count in cluster-based WSNs, the following definition is provided for the *Inherent Transmission Count* (*ITC*):

*Definition 1: Inherent Transmission Count (ITC) represents the total number of transmissions in a cluster-based WSN when all the nodes send a packet to the sink node according to a predetermined transmission strategy.*

*ITC* is composed of intra-cluster and inter-cluster transmission counts. The following theorem characterizes the relationship between *CR* and *ITC*:

*Theorem 1: For a given routing strategy and a clustering scheme in a cluster-based WSN, ITC is a convex function of CR for the m2s and m2m data propagation cases.*

*Proof:* The data propagation models *m2s* and *m2m* employ multi-hop transmission within a cluster. Therefore, the expected number of transmissions within a cluster needs to be first analyzed.

As stated in Sec. III-A, a cluster can be regarded as a Voronoi cell [20], [21]. Foss and Zuyev [21] analyzed the geometrical properties of a Voronoi cell (i.e., a cluster) in polar coordinates, and assumed that a CH is in 0 point. One of the important results they obtained is the expected number of nodes in a Voronoi cell, $E[N_{tot}]$, which is given as (See [21] for a complete proof of Eq. (4))

$$E[N_{tot}] = \lambda_{CM} 2\pi \int_0^{\infty} l e^{-\lambda_{CH}\pi l^2} dl, = \frac{\lambda_{CM}}{\lambda_{CH}}, \tag{4}$$

where $l$ denotes the radius of a cluster. In Eq. (4), $E[N_{tot}]$ is derived by integrating $2\pi l \lambda_{CM} e^{-\lambda_{CH}\pi l^2} dl$, where $2\pi l dl$ is the area element and $e^{-\lambda_{CH}\pi l^2}$ is the probability of a node belongs to the CH.

The same method is applicable for calculating the number of nodes located in the $i$-th hop. For the analysis, the integration interval $(0, \infty+)$ can be subdivided into the minimum transmission range of CM, $r_{min}$. Therefore, a cluster can be regarded as dividing it into $k$ ($k \to \infty+$) doughnut-shaped regions where each region has a width equal to $r_{min}$. Let $E[N^i_{CM}]$ represent the number of nodes in the $i$-th doughnut. Based on Eq. (4), $E[N^i_{CM}]$ can be derived as

$$E[N^i_{CM}] = \lambda_{CM} 2\pi \int_{(i-1)r_{min}}^{ir_{min}} l e^{-\lambda_{CH}\pi l^2} dl, = \frac{\lambda_{CM}}{\lambda_{CH}} (e^{-\lambda_{CH}\pi((i-1)r_{min})^2} - e^{-\lambda_{CH}\pi(ir_{min})^2}). \tag{5}$$

Eq. (5) satisfies $\sum_{i=1}^{k} E[N^i_{CM}] = E[N_{tot}]$ when $k \to \infty+$, and the complete proof of Eq. (5) is given in the Appendix. In addition, simulation results that validate the approximation efficiency of Eq. (5) are presented in Sec. V-A. Since the sensor nodes are assumed to be densely deployed, the transmission hop-count of the node in the $i$-th doughnut can be approximated by $i$ hops, and the expected total transmission count of the $i$-th doughnut is represented as $i \cdot E[N^i_{CM}]$. The total transmission count in a cluster $E[H]$ is a cumulative function of $i$ from 0 to $k$ given by the following equation:

$$\begin{aligned} E[H] &= \sum_{i=1}^{k} i\, E[N^i_{CM}] \\ &= \frac{\lambda_{CM}}{\lambda_{CH}} (1 + \sum_{i=1}^{k} e^{-\lambda_{CH}\pi(ir_{min})^2}) \\ &= \frac{\lambda_{CM}}{\lambda_{CH}} \sum_{i=0}^{k} e^{-\lambda_{CH}\pi(ir_{min})^2}. \end{aligned} \tag{6}$$

There are $N \cdot p$ clusters in the network; therefore the total expected transmission count $E[H_{tot}] = NpE[H]$, and it is given by

$$E[H_{tot}] = Np \frac{\lambda_{CM}}{\lambda_{CH}} \sum_{i=0}^{k} e^{-\lambda_{CH}\pi(ir_{min})^2}, \tag{7}$$

where $k \to \infty$. However, the time calculation for $k \to \infty+$ is time consuming and not necessary because $\lim_{k\to\infty+} e^{-\lambda_{CH}\pi(kr_{min})^2} = 0$, which means that when $k \to \infty$ the node is more likely to be within the range of other CHs. In actuality, if a node is not within the range of a cluster, $l$, the probability $e^{-\lambda_{CH}\pi(ir_{min})^2} \to 0$. Therefore, $k$ in Eq. (7) can be approximated by $\lceil l/r_{min} \rceil$. Note that both the shape and radius of a cluster is random; therefore, the average radius of a cluster $l$ is also a random value. In order to obtain the expected radius of a cluster, $E[l]$, the result from [21] is utilized, which showed that the total direct link length of a cluster is $E[L_{tot}] = \lambda_{CM}/2\lambda_{CH}^{3/2}$. After obtaining $E[L_{tot}]$ and $E[N_{tot}]$, $E[l]$ can be derived as follows:

$$E[l] = \frac{E[L_{tot}]}{E[N_{tot}]} = \frac{1}{\sqrt{4\lambda_{CH}}} = \sqrt{\frac{A}{4Np}}. \tag{8}$$

Since $k = \lceil E(l)/r_{min} \rceil = \lceil \sqrt{\frac{A}{4Nr_{min}^2 p}} \rceil$, substituting $\lambda(1-p)$ for $\lambda_{CM}$ and $\frac{(1-p)}{p}$ for $\frac{\lambda_{CM}}{\lambda_{CH}}$ into Eq. (7) yields the total transmission count in $N \cdot p$ clusters, $E[H_{tot}(p)]$, given as

$$E[H_{tot}(p)] = N(1-p) \sum_{i=0}^{\lceil \sqrt{\frac{A}{4Nr_{min}^2 p}} \rceil} e^{-\lambda p\pi(ir_{min})^2}. \tag{9}$$

Next, the *ITC* between CHs and the sink node is analyzed. For the *m2s* case, the total transmission count $E[H'_{tot}]$ is equal to the number of CHs because they directly transmit both the generated and received data to the sink node. Thus, the expected *ITC* for the *m2s* case, $E[ITC_{m2s}(p)]$, is given as

$$E[ITC_{m2s}(p)] = N(1-p) \sum_{i=0}^{\lceil \sqrt{\frac{A}{4Nr_{min}^2 p}} \rceil} e^{-\lambda p\pi(ir_{min})^2} + Np. \tag{10}$$

For the *m2m* case, CHs transmit packets to the sink node using multi-hop; therefore, the *ITC* between CHs and the sink node can be derived using the same method for the intra-cluster case. However, the densities of CMs and CHs need to be replaced by the density of CHs and the sink node,

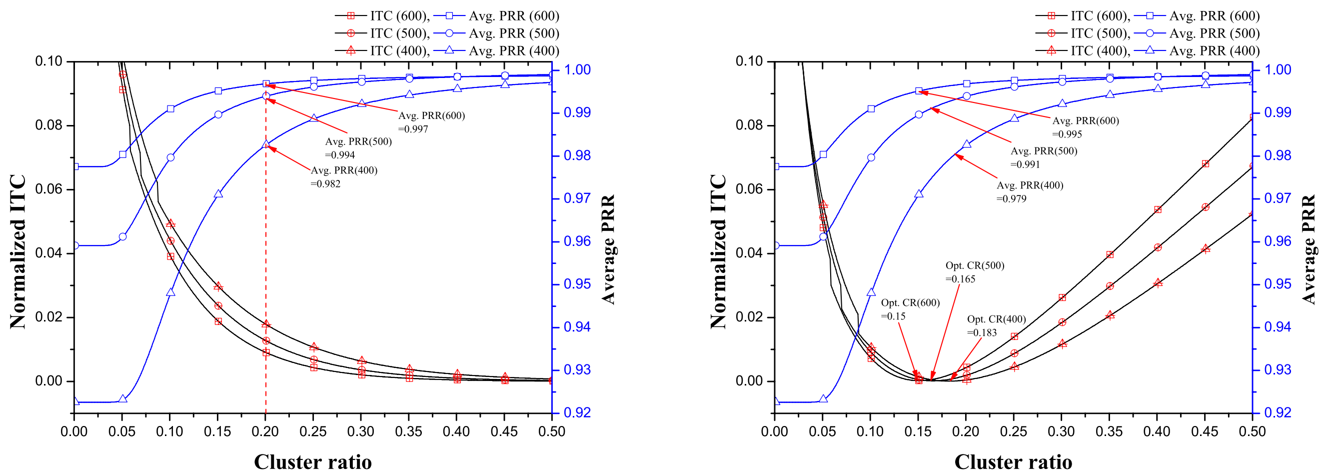


(a) (b)

Fig. 2. The impact of Cluster Ratio on normalized *ITC* and *PRR* ($k = 3.3$ and $r_{min} = 10$ m). (a) *m2s* case. (b) *m2m* case.

which are denoted by $\lambda'_{CH} = \lambda p$ and $\lambda_{sink} = \frac{1}{A}$, respectively. Based on Eq. (5), the transmission count between CHs and the sink node, $E[H_{tot}(p)^{'}]$, is given by

$$E[H_{tot}(p)^{'}] = \frac{\lambda'_{CH}}{\lambda_{sink}} \sum_{i=0}^{\lceil \frac{R}{r} \rceil} e^{-1/A\pi(ir)^2} = Np \sum_{i=0}^{\lceil \frac{R}{r} \rceil} e^{-1/A\pi(ir)^2}, \tag{11}$$

where $r$ and $R$ denote the transmission range of CH and the network radius, respectively. Based on this, the expected *ITC* for the *m2m* case, $E[ITC_{m2m}(p)]$, can be derived as

$$E[ITC_{m2m}(p)] = N(1-p) \sum_{i=0}^{\lceil \sqrt{\frac{A}{4Nr_{min}^2 p}} \rceil} e^{-\lambda p \pi (ir_{min})^2} + Np \sum_{i=0}^{\lceil \frac{R}{r} \rceil} e^{-1/A\pi(ir)^2}. \tag{12}$$

Therefore, *ITC* for both *m2s* and *m2m* cases can be determined based on the cluster ratio $p$ and the static network parameters, i.e., node density $\lambda$, network area $A$, and transmission ranges $r$ and $r_{min}$.

The convexity of Eqs. (10) and (12) can be proved by second-order conditions. In Eq. (10), the terms $N(1-p)$ (when $i = 0$) and $Np$ are linear functions, which have both concave and convex properties. Let $f(p) = e^{-\lambda p \pi (ir_{min})^2}$ for $0 < i \le \lceil \sqrt{\frac{A}{4Nr_{min}^2 p}} \rceil$, then the second-order of $f(p)$ is given by the following equation:

$$f^{''}(p) = (1-p)N(\lambda \pi r_{min}^2 i^2)^2 e^{-\lambda p \pi (ir_{min})^2} + 2N\lambda \pi r_{min}^2 i^2 e^{-\lambda p \pi (ir_{min})^2}, \tag{13}$$

where $0 < p < 1$. Eq. (13) shows that the condition $f^{''}(p) > 0$ is always satisfied for any value of $i$; therefore, $f(p)$ is a convex function for $0 < p < 1$.

Based on the above results, Eq. (10) is a nonnegative weighted sum of convex functions that preserves convexity of functions; therefore, it can be proved that it is a convex function. The convexity of Eq. (12) can be proved in a similar fashion, and thus the proof is complete. ■

Theorem 1 shows an important relationship between cluster ratio $p$ and *ITC*, and it indicates that there exists an optimized $p$ to minimize *ITC*. Fig. 2a and Fig. 2b show the *ITC* values as a function of $p$ for the *m2s* and *m2m* cases, respectively. The results in these figures show that for the *m2m* case, Eq. (12) is strictly convex, and there is only one optimum solution for $p$. However, for the *m2s* case, Eq. (10) is not a strictly convex function; therefore, an additional restricted condition is needed to determine an appropriate $p$.

## *B. Optimal Cluster Ratio for Maximizing Communication Reliability*

The optimum $p$ for *ITC* does not necessarily guarantee energy efficiency because packet retransmissions will decrease the performance of the optimized solutions. Therefore, this subsection explores an energy efficient solution from the perspective of communication reliability, and analyzes the trade-off between minimizing *ITC* and maximizing *PRR* in cluster-based WSNs.

Given a network, let $\mathbb{P}$ indicate a Bernoulli random value. If a packet is successfully received, $\mathbb{P} = 1$; otherwise, $\mathbb{P} = 0$. Assuming $\mathbb{P}$ is independent and identically distributed (iid) and according to the weak law of large numbers, *PRR* can be statistically approximated by the following equation:

$$\mathbb{P} = PRR = (1 - \mathbb{P}_b)^{8F}, \tag{14}$$

where $F$ indicates frame size in bytes and $\mathbb{P}_b$ is bit error rate, which is generally defined by following equation [26]:

$$\mathbb{P}_b(\gamma) = \alpha_M Q(\sqrt{\beta_M \gamma}), \tag{15}$$

where $\gamma$ indicates Signal to Noise Ratio (SNR), $Q(\cdot)$ denotes the Gaussian $Q$-function, and $\alpha_M$ and $\beta_M$ are determined by the type of approximation and modulation.

Eq. (15) shows that the bit error rate is a function of $\gamma$. On the receiver side, $\gamma = r_{ss} - N_{floor}$, where $r_{ss}$ is the receiver sensitivity and $N_{floor}$ is the noise floor. During signal propagation, the signal power decreases as distance increases. This phenomenon is statistically modeled using the path loss model $P_L(d)$ defined in Sec. III-C. For the transmission power $P_{tx}$, the condition $r_{ss} \geq P_{tx} - P_L(d)$ must be guaranteed at the receiver. Thus, $r_{ss}$ can be approximated as $P_{tx} - P_L(d)$. Let $\overline{P_L(d)}$ denote the average path loss in a cluster, i.e., $r_{ss} = P_{tx} - \overline{P_L(d)}$ and $\overline{\gamma} = \theta - \overline{P_L(d)}$, where $\theta = P_{tx} - N_{floor}$. Then, the average *PRR*, $\overline{PRR}$, can be derived by substituting $\overline{\gamma}$ for $\gamma$ for Eq. (15) as given below:

$$\overline{PRR}(d) = (1 - \alpha_M Q\sqrt{\beta_M(\theta - \overline{P_L(d)})})^{8F}. \quad (16)$$

Since a CH is assumed to provide reliable communication using higher transmission power or enhanced low-power long-distance RF module (such as low-power Bluetooth), $\overline{PRR}$ should be optimized for intra-cluster. Within a cluster, CMs can be in one of two possible states: ideal-state and isolated-state. In the ideal state, at least one neighbor node is located within the transmission range of a CM. In contrast, in the isolated-state, there are no relay nodes located within the transmission range of a CM, and thus it has to directly communicate with the CH. The communication reliability of CMs that are in the ideal-state can be guaranteed because the relay nodes are located within their transmission range. On the other hand, CMs that are in the isolated-state will incur many packet retransmissions. Therefore, $\overline{PRR}$ must be derived after obtaining the probabilities that a node will stay in either the ideal-state or the isolated-state.

In the Poisson 2-D model, the cumulative distribution function (CDF) that the distance of a neighbor node $d$ is smaller than $r_{min}$ is $F(d \leq r_{min}) = 1 - e^{-\pi\lambda r_{min}^2}$. Based on this, the probability that a node remains in the isolated-state can be derived as $1 - F(d \leq r_{min}) = e^{-\pi\lambda r_{min}^2}$, and thus, the probability that a node is in the ideal-state is $1 - e^{-\pi\lambda r_{min}^2}$. For an isolated node, it has to directly communicated with the CH over distance $E[l]$ defined in Eq. (8). Based on these results and Eq. (16), the average *PRR* in a cluster is obtained as follow:

$$\begin{aligned}\overline{PRR}(p) &= F(d \leq r_{min}) + (1 - F(d \leq r_{min}))PRR_{isolated} \\ &= (1 - e^{-\pi\lambda r_{min}^2}) \\ &\quad + e^{-\pi\lambda r_{min}^2}(1 - \alpha_M Q(\sqrt{\beta_M(\theta - P_L(\sqrt{\frac{A}{4Np}}))})^{8F}),\end{aligned} \quad (17)$$

where $PRR_{isolated}$ denotes *PRR* of the isolated node.

Eq. (17) shows that if the modulation scheme as well as $Q(\cdot)$ are known, the average *PRR* can be optimized in a cluster by determining the appropriate cluster ratio $p$.

### C. Optimal Cluster Ratio

The aforementioned analysis shows that an appropriate $p$ potentially improves not only *ITC* but also $\overline{PRR}$. However, the results obtained from Theorem 1 and Eq. (17) are independently derived. Therefore, this subsection presents a joint optimization method that optimizes both *ITC* and $\overline{PRR}$ simultaneously.

Without loss of generality, let $\alpha_M = 1$ and $\beta_M = 1$ (which is valid when the nodes use the FSK modulation scheme) to compare the impact of $p$ on *ITC* and $\overline{PRR}$. This yields the following bit error rate:

$$\mathbb{P}_b(\gamma) = Q(\sqrt{\gamma}) = \frac{1}{2}e^{-\frac{B_n\gamma}{2\eta}}, \quad (18)$$

where $B_n$ and $\eta$ denote the noise bandwidth and transmission rate, respectively. Substituting Eq. (18) into Eq. (17) results in the following equation for average *PRR*:

$$\begin{aligned}\overline{PRR}(p) &= (1 - e^{-\pi\lambda r_{min}^2}) \\ &\quad + (1 - \frac{1}{2}e^{-\frac{B_n}{2\eta}(\theta' - 10k\log_{10}\sqrt{\frac{A}{4Np}})})^{8F},\end{aligned} \quad (19)$$

where $\theta' = \theta - 20\log_{10}(\frac{4\pi}{\omega})$ and $\omega$ denotes the wave length.

Fig. 2 shows the impact of $p$ and node density on *ITC* and $\overline{PRR}$ for the *m2s* (Fig. 2a) and *m2m* (Fig. 2b) cases. As mentioned in Sec. IV-B, *ITC* for the *m2s* case is not a strictly convex function. This property can be observed from Fig. 2a, where the normalized *ITC* converges as $p$ increases for the *m2s* case. Based on this property, the lower bound of the joint optimization solution $p^*$ can be obtained for the *m2s* case[1] with the jointly restricted condition, which is the minimum required communications reliability $PRR_{req} = 98\%$. According to the analytical results in Fig. 2a, the joint optimization value for $p^*$ that optimizes *ITC* and guarantees $PRR_{req}$ for various node densities is 0.2.

However, in the *m2m* case, it is difficult to determine the joint optimization solution $p^*$ with a restricted bound of $PRR_{req}$ to simultaneously optimize *ITC* and $\overline{PRR}$. The reason is that the optimized $p^*$ maximizes $\overline{PRR}$ in a cluster by decreasing its area and the distance between CMs and CH. At the same time, the optimized $p^*$ causes the network to be divided into more clusters and thus increases the transmission overhead.

For the *m2m* case, a low $\overline{PRR}$ will result in excessive packet retransmissions within a cluster. The retransmission count can be derived as $E[H_{tot}(p)] \times (1 - \overline{PRR}(p))$, where $E[H_{tot}(p)]$ is given by Eq. (9), and $\overline{PRR}(p)$ is given by Eq. (19). On the other hand, the total number of transmissions is the sum of *ITC* and the number retransmissions. Therefore, the problem of independently optimizing *ITC* and retransmission count is converted into a problem of minimizing the total transmission count. This is formulated by the following joint optimization function $p^*$:

$$\begin{aligned}p^* = \arg\min_{p\in(0,1)} &(E[H_{tot}(p)] \times (2 - \overline{PRR}(p)) \\ &+ E[H_{tot}(p)^{'}]).\end{aligned} \quad (20)$$

The objective function in Eq. (20) consists of the sum of *ITC* and retransmission count for the intra-cluster transmission (the first term) and *ITC* for the inter-cluster transmission (the second term), where the argument $p$ is in the interval $(0, 1)$.

[1] In order to distinguish the joint optimization from the normal optimization, notation $p^*$ is used to denote the result of the joint optimization.

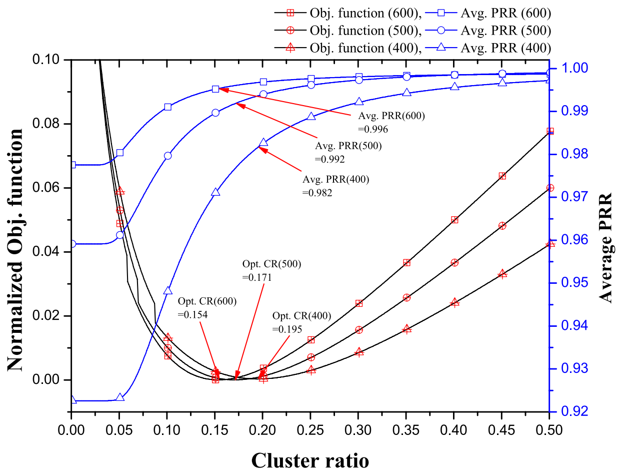


Fig. 3. Results of joint optimization.

Therefore, $p^*$ is obtained that simultaneously minimizes the network transmission hop-count and maximizes $\overline{PRR}$ with constant time $O(1)$. Fig. 3 shows the results of Eq. (20), which indicate that the optimal $p^*$ values are 0.195, 0.171, and 0.154 for node densities of 400, 500, and 600, respectively, and the derived $p^*$ can guarantee 98% communication reliability.

## V. Performance Evaluation

This section compares the performance of the proposed method for determining optimal $p^*$ values against the methods presented in [16]–[18]. The simulated area has a radius of 100 *m* with the sink node located at the center, and the number of randomly deployed nodes are 400, 500, and 600. CHs are also randomly selected based on the given cluster ratio $p$. Each node selects the closest CH and performs either multi-hop or direct transmission depending on the communication distance. Moreover, each sensor node generates 50-byte packets at a transmission rate of 50 kbps. The network occupies 915 MHz frequency band, and transmission power is set to 0 dBm and −25 dBm for intra-cluster and inter-cluster transmission, respectively. The simulator for the performance evaluation is implemented in C.

### *A. Validation of the Approximation Efficiency*

This subsection validates the approximation efficiency of Eq. (5) using simulation. Fig. 4 shows the average number of nodes in $i$-th doughnut, where solid lines denote the simulation results (which are averages of 200 runs) and dash lines denote the calculated results of Eq. (5). Eq. (5) takes the $i$-th hop as well as the density of cluster head and cluster members, which is based on $p$, as input parameters and calculates the results for different values of $p$, i.e., 0.08, 0.12, 0.16, 0.2, and 0.24.

The following two observations can be made from Fig. 4. The first is the impact of node density on the approximation efficiency. Our results show that the approximation accuracy increases as node density increases. The second is that the approximation error can be ignored if $p$ is sufficiently large. For example, although the node density is low in Fig. 4a, the approximation results are close to the simulation results when $p > 0.08$, and the proposed optimization point, $p^*$, is greater than 0.08 as presented in Sec. IV-C (i.e., $p^* = 0.2$ in the *m2s* case and $p^* = \{0.195, 0.171, 0.154\}$ in the *m2m* case). Therefore, the approximation suffers from only few interference errors.

### *B. Performance of the Proposed Joint Optimization*

This subsection compares the performance of the optimized $p$ based on the *ITC* function in Eq. (12) and the proposed joint optimization function in Eq. (20). Based on Eqs. (12) and (20), the optimal $p$ and $p^*$ for the three node densities are {0.183, 0.165, 0.15} and {0.195, 0.171, 0.154}, respectively. In order to provide a fair performance comparison, the data generation in the simulation is set so that each node in the network sequentially generates one packet and sends it to the sink node.

Fig. 5 compares the *ITC* values obtained from the proposed joint optimization scheme and optimizing only the *ITC* function for various node densities. The numbers on histograms are used to indicate the optimal $p$ which are obtained by the analytic models. These results show that the optimal $p^*$ obtained using the joint optimization scheme can reduce *ITC* by 2.18%, 1.68%, and 1.14% compare to $p$ obtained from only optimizing the *ITC* function. Fig. 6 shows that the communication reliability is also enhanced by the joint optimization. The reason for this is that the proposed method simultaneously optimizes the network *ITC* and *PRR*, and thus, higher *PRR* is guaranteed and the number of retransmissions is effectively reduced resulting in lower *ITC*. Therefore, these results verify that the proposed joint optimization leads to a more energy efficient network.

### *C. Comparison With Existing Optimal Cluster Ratio Analytical Models*

This subsection compares the proposed joint optimization with the existing analytical models by Kumar *et al.* [16] and Kumar [17] and Bandyopadhyay and Coyle [18]. According to their results, the optimal $p$ values are {0.06, 0.054, 0.049} [16], [17], and {0.101, 0.093, 0.087} [18] for the three node densities.

Fig. 7 shows the network *ITC* results for different optimum $p$ and $p^*$ values and node densities. The figure shows that the cluster ratio optimization techniques proposed in [16]–[18] do not minimize the network *ITC*. The reason is that the analytic model in [16] and [17] is an extension of LEACH for multi-hop communications, which does not take into account the important factors in energy efficiency, which are *ITC* and *PRR*. The optimization technique proposed by Bandyopadhyay and Coyle [18] shows better performance than the one provided in [16] and [17], and this is because their analysis is performed with minimizing the network *ITC* in mind. However, there is a performance gap between the optimal $p^*$ provided by the proposed joint optimization scheme and the one by Bandyopadhyay *et al.* This gap is caused by their estimation errors, and is also related to the fact that they do not take communication reliability into consideration.

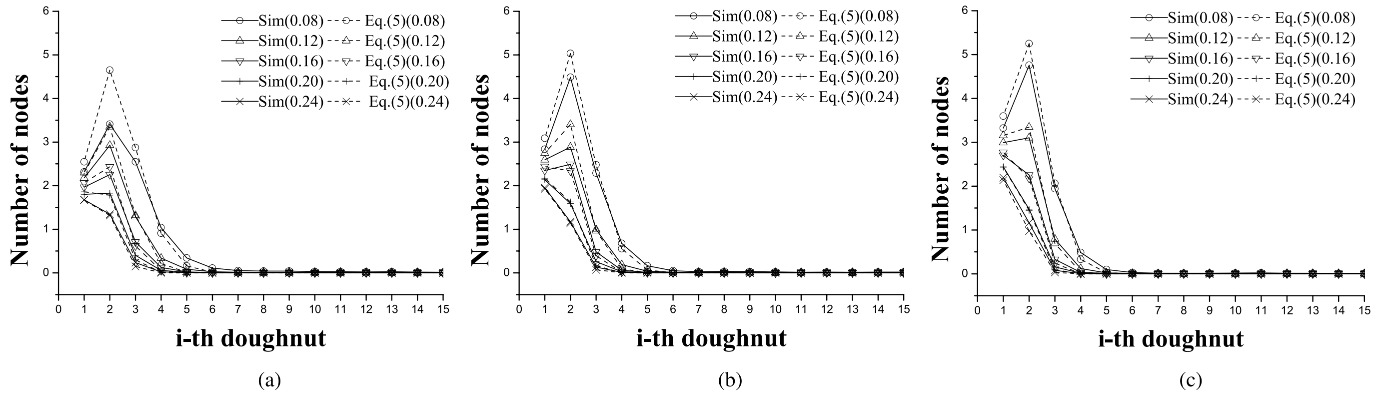


Fig. 4. Comparison of simulation and approximation results ($r_{min} = 10$ m and $p = \{0.08, 0.12, 0.16, 0.2, 0.24\}$). (a) Number of nodes deployed is 400. (b) Number of nodes deployed is 500. (c) Number of nodes deployed is 600.

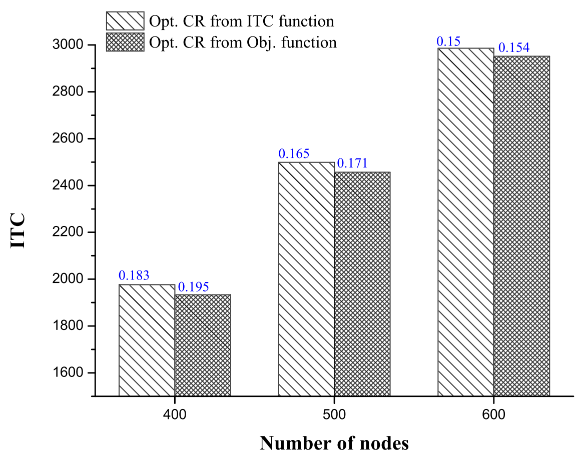


Fig. 5. Comparison of the network *ITC* for different node densities.

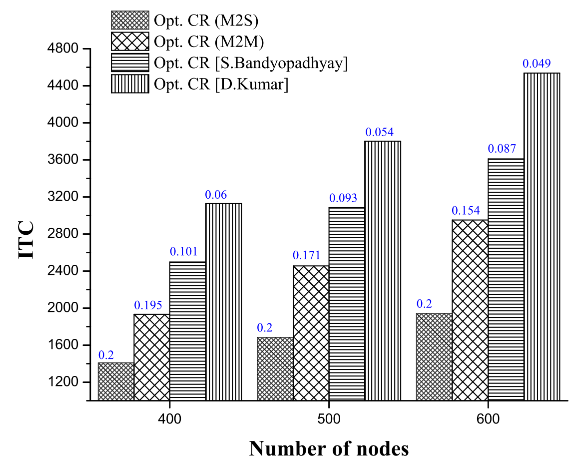


Fig. 7. Network *ITC*.

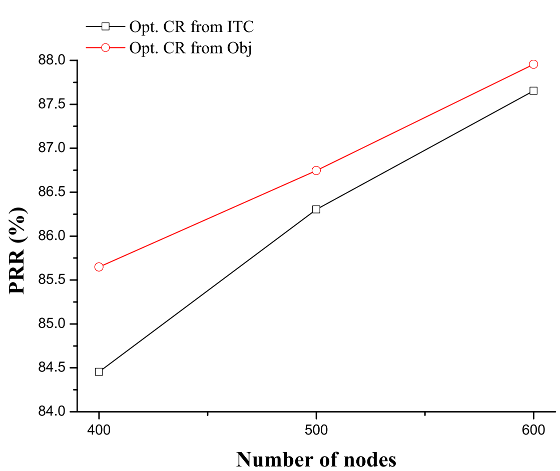


Fig. 6. Comparison of the average *PRR* for different node densities.

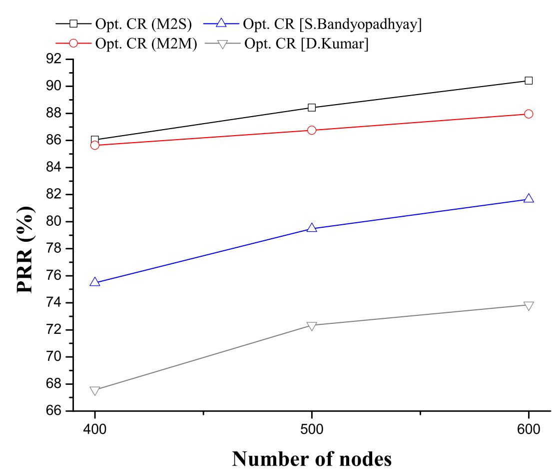


Fig. 8. Average *PRR*.

Fig. 8 shows the average *PRR* for the three node densities. This figure shows that the existing optimization techniques result in low average *PRR*, and this will cause a lot of packet retransmissions and extra energy dissipation. With an improper choice of $p$, the average *PRR* will be low as shown in the mathematical analysis results in Fig. 2, and it becomes worse as the hop-count increases. As shown in Fig. 8, the average *PRR* can be improved by increasing the node density. The reason is that if nodes are more densely deployed, the probability of maintaining good communication links increases. However, simply increasing node density is not feasible in most applications. Therefore, properly setting

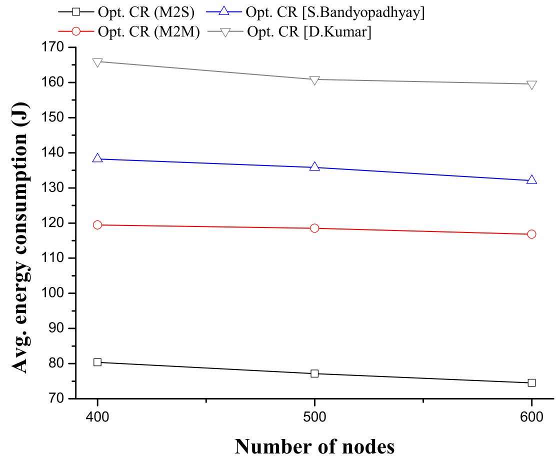


Fig. 9. Average energy consumption.

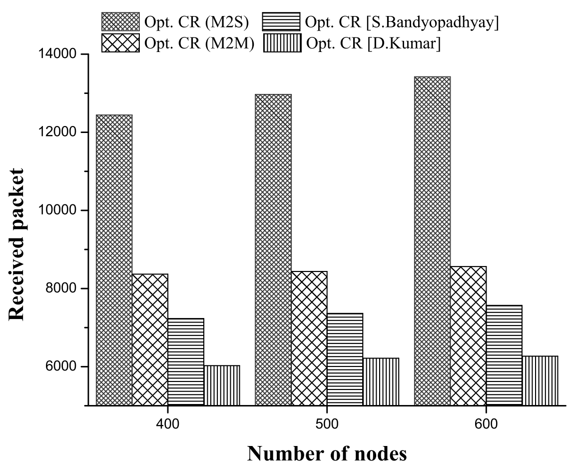


Fig. 10. Received packet before FND.

the $p$ value is a more efficient way to improve the network *PRR* and enhance network energy efficiency.

These simulation results also show that the performance improvement in *m2s* is higher than *m2m*. This is because low-power, long-distance RF module is assumed in *m2s*; therefore, the connection between CHs and the sink node is ideal, and thus *ITC* is equal to the number of CHs, which is lower than for multi-hop communications.

### D. Network Life Time

This subsection studies the impact of various cluster ratio optimization techniques on the network energy efficiency. In order to evaluate energy consumption, simulation is performed for 100 iterations, and in each iteration, each sensor node sends 1000 packets to the sink node. In this paper, the network life time is defined as the time until the FND (First Node "Dead") [1]. The initialized energy is set to 10 J, and the abstract time is represented by a more specific metric, which is the number of packets received at the sink node before FND.

Fig. 9 shows that the proposed joint optimization technique significantly reduces the energy consumption of sensor nodes, which clearly indicates the benefits of optimizing both *ITC* and *PRR*.

Fig. 10 shows that proposed analytical model outperforms existing schemes in terms of network lifetime. By setting optimal $p^*$, the number of received packets is approximately $14\% \sim 39\%$ higher than the methods in [16]–[18] for the *m2m* case. The results for the *m2s* case is significantly better than the existing methods (by at least 72%) because data from each sensor node is aggregate at a CH and then transmitted directly to the sink node.

Our study shows that the proposed joint optimization technique significantly improves the network energy efficiency in term of *ITC* and *PRR*, and increases the network lifetime. Another notable result is that energy efficiency of the *m2s* case is better than the *m2m* case. This is because even though more energy is consumed during long distance transmissions, the benefits of lower *ITC* and higher average *PRR* lead to longer network life time than the *m2m* case.

## VI. CONCLUSION

This paper presented a novel analytical model to analyze the optimal *CR* for cluster-based WSNs to enhance the network energy efficiency. The impact of *CR* on the network performance was analyzed without any specific assumptions about energy models and network environment. Furthermore, the analysis considers various data propagation models. Therefore, the analysis is applicable to generic cluster-based WSNs. Based on the analytic model, a joint optimization scheme was proposed to improve the network energy efficiency by simultaneously optimizing *ITC* and *PRR*. The performance of the optimal *CR* derived using the proposed joint optimization scheme was validated through simulations. Our simulation results clearly showed the benefits of the optimal *CR* over existing optimization methods in terms of *PRR* and energy efficiency. Our future plan is to extend the proposed analytic model to consider other issues such as impact of data aggregation scheme and specific application environments.

## APPENDIX
## PROOF OF FORMULA (5)

In a given cluster, $\mathrm{CH}_i$, the expected number of CMs within radius $r'$, $E[N_{r'}]$, can be derived as

$$E[N_{r'}] = \int_0^{r'} \lambda_{CM} 2\pi l \mathbf{P}(CM_j \in CH_i) dl, \tag{21}$$

where $\mathbf{P}(\cdot)$ denotes a Plam distribution. The sensor nodes are deployed within the network based on a homogeneous Poisson point process, and $\mathrm{CM}_j$ belongs to $\mathrm{CH}_i$ if and only if a disc with the radius $l$ around $CM_i$ does not contain any other CHs. Therefore, $\mathbf{P}(CM_j \in CH_i) = e^{-\lambda_{CH}\pi l^2}$ and Eq. (21) can be rewritten as shown below:

$$\begin{aligned} E[N_{r'}] &= \lambda_{CM} 2\pi \int_0^{r'} l e^{-\lambda_{CH}\pi l^2} dl, \\ &= \frac{\lambda_{CM}}{\lambda_{CH}}(1 - e^{-\lambda_{CH}\pi r'^2}). \end{aligned} \tag{22}$$

When $r' \rightarrow \infty$, $e^{-\lambda_{CH}\pi r'^2} = 0$ and thus $E[N_{r'}] = E[N_{tot}] = \frac{\lambda_{CM}}{\lambda_{CH}}$. (A complete proof of Eq. (4) (or Eq. (22)) is given in [21].)

According to Eq. (22), the expected number of CMs within radiuses $r_{min}$ and $2r_{min}$ are $\frac{\lambda_{CM}}{\lambda_{CH}}(1 - e^{-\lambda_{CH}\pi r_{min}^2})$ and $\frac{\lambda_{CM}}{\lambda_{CH}}(1 - e^{-\lambda_{CH}\pi (2r_{min})^2})$, respectively. Suppose the region of the $i$-th donut is defined as $\pi(ir_{min})^2 - \pi((i-1)r_{min})^2$, then the expected number of CMs in the 2-nd donut ($i = 2$), $E[N_{CM}^2]$, is given as

$$\begin{aligned} E[N_{CM}^2] &= \frac{\lambda_{CM}}{\lambda_{CH}}(1 - e^{-\lambda_{CH}\pi(2r_{min})^2}) \\ &\quad - \frac{\lambda_{CM}}{\lambda_{CH}}(1 - e^{-\lambda_{CH}\pi r_{min}^2}) \\ &= \frac{\lambda_{CM}}{\lambda_{CH}}(e^{-\lambda_{CH}\pi r_{min}^2} - e^{-\lambda_{CH}\pi(2r_{min})^2}). \end{aligned} \tag{23}$$

Using the same method that analyzes the expected number for the simple case (where $i = 2$), Eq. (23) can be normalized to a general case for a non-negative integer, $i$.

$$\begin{aligned} E[N_{CM}^i] &= \frac{\lambda_{CM}}{\lambda_{CH}}(1 - e^{-\lambda_{CH}\pi(ir_{min})^2}) \\ &\quad - \frac{\lambda_{CM}}{\lambda_{CH}}(1 - e^{-\lambda_{CH}\pi((i-1)r_{min})^2}) \\ &= \frac{\lambda_{CM}}{\lambda_{CH}}(e^{-\lambda_{CH}\pi((i-1)r_{min})^2} - e^{-\lambda_{CH}\pi(ir_{min})^2}). \end{aligned} \tag{24}$$

The calculation of Eq. (24) can be represented with a simple integral operation, and then Eq. (5) is obtained as below.

$$\begin{aligned} E[N_{CM}^i] &= \lambda_{CM} 2\pi \Big(\int_0^{ir_{min}} l e^{-\lambda_{CH}\pi l^2} dl \\ &\qquad - \int_0^{(i-1)r_{min}} l e^{-\lambda_{CH}\pi l^2} dl\Big), \\ &= \lambda_{CM} 2\pi \int_{(i-1)r_{min}}^{ir_{min}} l e^{-\lambda_{CH}\pi l^2} dl. \end{aligned} \tag{25}$$

## REFERENCES


[1] W. B. Heinzelman, A. P. Chandrakasan, and H. Balakrishnan, "An application-specific protocol architecture for wireless microsensor networks," *IEEE Trans. Wireless Commun.*, vol. 1, no. 4, pp. 660–670, Oct. 2002.

[2] I. F. Akyildiz, W. Su, Y. Sankarasubramaniam, and E. Cayirci, "A survey on sensor networks," *IEEE Commun. Mag.*, vol. 40, no. 8, pp. 102–114, Aug. 2002.

[3] A. A. Abbasi and M. Younis, "A survey on clustering algorithms for wireless sensor networks," *Comput. Commun.*, vol. 30, nos. 14–15, pp. 2826–2841, Oct. 2007.

[4] Y.-K. Huang, A.-C. Pang, P.-C. Hsiu, W. Zhuang, and P. Liu, "Distributed throughput optimization for ZigBee cluster-tree networks," *IEEE Trans. Parallel Distrib. Syst.*, vol. 23, no. 3, pp. 513–520, Mar. 2012.

[5] H. Lu, J. Li, and M. Guizani, "Secure and efficient data transmission for cluster-based wireless sensor networks," *IEEE Trans. Parallel Distrib. Syst.*, vol. 25, no. 3, pp. 750–761, Mar. 2014.

[6] M. Noori and M. Ardakani, "Lifetime analysis of random event-driven clustered wireless sensor networks," *IEEE Trans. Mobile Comput.*, vol. 10, no. 10, pp. 1448–1458, Oct. 2011.

[7] H. Shen, Z. Li, L. Yu, and C. Qiu, "Efficient data collection for large-scale mobile monitoring applications," *IEEE Trans. Parallel Distrib. Syst.*, vol. 25, no. 6, pp. 1424–1436, Jun. 2014.

[8] H. Yang and B. Sikdar, "Optimal cluster head selection in the LEACH architecture," in *Proc. IEEE Int. Perform., Comput., Commun. Conf. (IPCCC)*, Apr. 2007, pp. 93–100.

[9] Y. P. Chen, A. L. Liestman, and J. Liu, "Energy-efficient data aggregation hierarchy for wireless sensor networks," in *Proc. IEEE Int. Conf. Quality Service Heterogeneous Wired/Wireless Netw. (QSHINE)*, Aug. 2005, p. 7.

[10] B. Chen, Y. Zhang, Y. Li, X. Hao, and Y. Fang, "A clustering algorithm of cluster-head optimization for wireless sensor networks based on energy," *Inf. Comput. Sci.*, vol. 8, no. 11, pp. 2129–2136, Nov. 2011.

[11] O. Younis and S. Fahmy, "HEED: A hybrid, energy-efficient, distributed clustering approach for ad hoc sensor networks," *IEEE Trans. Mobile Comput.*, vol. 3, no. 4, pp. 366–379, Oct./Dec. 2004.

[12] D. Wei, Y. Jin, S. Vural, K. Moessner, and R. Tafazolli, "An energy-efficient clustering solution for wireless sensor networks," *IEEE Trans. Wireless Commun.*, vol. 10, no. 11, pp. 3973–3983, Nov. 2011.

[13] Y. Jin, D. Wei, S. Vural, A. Gluhak, and K. M. Moessner, "A distributed energy-efficient re-clustering solution for wireless sensor networks," in *Proc. IEEE Global Commun. Conf. (GLOBECOM)*, Dec. 2011, pp. 1–6.

[14] S. V. Manisekaran and R. Venkatesan, "An adaptive distributed power efficient clustering algorithm for wireless sensor networks," *Amer. J. Sci. Res.*, no. 10, pp. 50–63, 2010.

[15] K. T. Kim, H. K. Yoo, B. H. Son, and H. Y. Youn, "An energy efficient clustering scheme for self-organizing distributed wireless sensor networks," in *Proc. IEEE Int. Conf. Comput. Inf. Technol. (CIT)*, Jun. 2010, pp. 1468–1473.

[16] D. Kumar, T. C. Aseri, and R. B. Patel, "EEHC: Energy efficient heterogeneous clustered scheme for wireless sensor networks," *Comput. Commun.*, vol. 32, no. 4, pp. 662–667, Mar. 2009.

[17] D. Kumar, "Performance analysis of energy efficient clustering protocols for maximising lifetime of wireless sensor networks," *IET Wireless Sensor Syst.*, vol. 4, no. 1, pp. 9–16, Mar. 2014.

[18] S. Bandyopadhyay and E. J. Coyle, "An energy efficient hierarchical clustering algorithm for wireless sensor networks," in *Proc. IEEE Int. Conf. Comput. Commun. (INFOCOM)*, vol. 3. Mar./Apr. 2003, pp. 1713–1723.

[19] R. Xie and X. Jia, "Transmission-efficient clustering method for wireless sensor networks using compressive sensing," *IEEE Trans. Parallel Distrib. Syst.*, vol. 25, no. 3, pp. 806–815, Mar. 2014.

[20] S. N. Chiu, D. Stoyan, W. S. Kendall, and J. Mecke, *Stochastic Geometry and Its Applications*, 3rd ed. New York, NY, USA: Wiley, 2013, ch. 10.

[21] S. G. Foss and S. A. Zuyev, "On a Voronoi aggregative process related to a bivariate Poisson process," *Adv. Appl. Probab.*, vol. 28, no. 4, pp. 965–981, 1996.

[22] Y. Tian, Z. Shu-Fang, and Y. Wang, "A distributed protocol for ensuring both probabilistic coverage and connectivity of high density wireless sensor networks," in *Proc. IEEE Wireless Commun. Netw. Conf. (WCNC)*, Mar./Apr. 2008, pp. 2069–2074.

[23] M. Khanjary, M. Sabaei, and M. R. Meybodi, "Critical density for coverage and connectivity in two-dimensional aligned-orientation directional sensor networks using continuum percolation," *IEEE Sensors J.*, vol. 14, no. 8, pp. 2856–2863, Aug. 2014.

[24] H. Cai, X. Jia, and M. Sha, "Critical sensor density for partial connectivity in large area wireless sensor networks," in *Proc. IEEE Int. Conf. Comput. Commun. (INFOCOM)*, Mar. 2010, pp. 1–5.

[25] *IEEE Standard for Information technology-Telecommunications and Information Exchange Between Systems-Local and Metropolitan Area Networks-Specific Requirements—Part 15.4: Wireless Medium Access Control (MAC) and Physical Layer (PHY) Specifications for Low-Rate Wireless Personal Area Networks (LR-WPAN)*, IEEE Standard 802.15.4-2006, 2006.

[26] A. Goldsmith, *Wireless Communications*. Cambridge, U.K.: Cambridge Univ. Press, 2005, ch. 6.


**Zilong Jin** (S'15) received the B.E. degree in computer engineering from the Harbin University of Science and Technology, China, in 2009, and the M.S. degree in computer engineering from Kyung Hee University, Korea, in 2011. He is currently pursuing the Ph.D. degree with the Department of Computer Engineering, Kyung Hee University, Korea. His interests include wireless sensor networks, mobile wireless networks, and cognitive radio networks.

**Dae-Young Kim** received the B.S. degree in electronics engineering, and the M.S. and Ph.D. degrees in computer engineering from Kyung Hee University, Korea, in 2004, 2006, and 2010, respectively. From 2010 to 2013, he was a member of the Research Staff with the Communication Research and Development Laboratory, LIG Nex1, Korea. From 2013 to 2015, he was a member of the Research Staff with Network Team, AirPlug, Inc., Korea. He was a Research Staff with the Gyeongbuk Institute of IT Convergence Industry Technology, Korea, in 2015. He is currently an Assistant Professor with the Department of Software Engineering, Changshin University, Korea. His research interests include mobile networking and computing, wireless sensor networks, and embedded systems.

**Jinsung Cho** (M'15) received the B.S., M.S, and Ph.D. degrees in computer engineering from Seoul National University, Korea, in 1992, 1994, and 2000, respectively. He was a Visiting Researcher with the IBM T. J. Watson Research Center, in 1998, and a member of the Research Staff with Samsung Electronics, from 1999 to 2003. He is currently a Professor with the Department of Computer Engineering, Kyung Hee University, Korea. His research interests include mobile networking and computing, embedded systems and software, and sensor and body networks.

**Ben Lee** received the B.E. degree in electrical engineering from the Department of Electrical Engineering, State University of New York (SUNY) at Stony Brook, in 1984, and the Ph.D. degree in computer engineering from the Department of Electrical and Computer Engineering, Pennsylvania State University, in 1991. He is currently a Professor of School of Electrical Engineering and Computer Science with Oregon State University. His research interests include wireless networks, embedded systems, computer architecture, multimedia systems, and parallel and distributed systems. He received the Loyd Carter Award for Outstanding and Inspirational Teaching and the Alumni Professor Award for Outstanding Contribution to the College and the University from the OSU College of Engineering, in 1994 and 2005, respectively. He also received the HKN Innovative Teaching Award from Eta Kappa Nu, School of Electrical Engineering and Computer Science, in 2008. He has been on the Program and Organizing Committees for numerous international conferences, including the 2003 International Conference on Parallel and Distributed Computing Systems, the 2005–2011 IEEE Workshop on Pervasive Wireless Networking, and the 2006, 2007, and 2009 IEEE International Conference on Pervasive Computing and Communications. He was also a Keynote Speaker at the 2014 International Conference on Ubiquitous Information Management and Communication. He is currently the Chair of the Social, P2P and Multimedia Networking, Services and Applications track for the 2016 IEEE Consumer Communications and Networking Conference.